LAWRENCE
LIVERMORE
NATIONAL
LABORATORY

UCRL-TR-218414

The Refuelable Zinc-air Battery: Alternative Techniques for Zinc and Electrolyte Regeneration

John F. Cooper, Roger Krueger

January 25, 2006

This work was performed under the auspices of the U.S. Department of Energy by University of California, Lawrence Livermore National Laboratory under Contract W-7405-Eng-48.

UCRL-TR-218414

(Same report released in 1996 as UCRL-ID-123927)

Final Report

ILZRO Program Number and Title:

ZB-1 Zinc-Air Batteries

April 15, 1996

for:

International Lead-Zinc Research Organization

P.O. Box 12036

Research Triangle Park

NC 27709-2036

Tel. (919) 361-4647

The Refuelable Zinc-Air Battery: Alternative Techniques for Zinc and Electrolyte Regeneration

John F. Cooper, Ph.D. (Principal Investigator) and Roger Krueger
Department of Chemistry and Materials Science, L-369
Lawrence Livermore National Laboratory • Livermore CA 94550

(Tel.) 510-423-6649
(Fax) 510-422-2118
Cooper3@LLNL.gov

Table Contents

Abstract

An investigation was conducted into alternative techniques for zinc and electrolyte regeneration and reuse in the refuelable zinc/air battery that was developed by LLNL and previously tested on a moving electric bus using cut wire. Mossy zinc was electrodeposited onto a bipolar array of inclined Ni plates with an energy consumption of 1.8 kWh/kg. Using a H_2-depolarized anode, zinc was deposited at 0.6 V (0.8 kA/m^2); the open circuit voltage was 0.45 V. Three types of fuel pellets were tested and compared with results for 0.75 mm cut wire: spheres produced in a spouted bed (UCB); coarse powder produced by gas-atomization (Noranda); and irregular pellets produced by chopping 1-mm plates of compacted zinc fines (Eagle-Picher, Inc.). All three types transported within the cell. The coarse powder fed continuously from hopper to cell, as did the compacted pellets (< 0.83 mm). Large particles (> 0.83 mm; Eagle-Picher and UCB) failed to feed from hopper into cell, being held up in the 2.5 mm wide channel connecting hopper to cell. Increasing channel width to ~3.5 mm should allow all three types to be used.

Energy losses were determined for shorting of cells during refueling. The shorting currents between adjacent hoppers through zinc particle bridges were determined using both coarse powder and chopped compressed zinc plates. A physical model was developed allowing scaling our results for electrode polarization and bed resistance Shorting was found to consume < 0.02% of the capacity of the cell and to dissipate ~0.2 W/cell of heat. Corrosion rates were determined for cut wire in contact with current collector materials and battery-produced ZnO-saturated electrolyte. The rates were 1.7% of cell capacity per month at ambient temperatures; and 0.08% of capacity for 12 hours at 57 °C.

The total energy conversion efficiency for zinc recovery using the hydrogen was estimated at 34% (natural gas to battery terminals)--comparable to fuel cells. Producing zinc shot was quoted at 1.5-3 ¢/lb above base price (52¢/lb, ASM) for super purity ingot.

Both the spouted-bed and the Eagle-Picher processes might conceivably be configured for fleet operation in user-owned and operated equipment located a the fleet's home base. This would eliminate the need for green-field industrial plants and fuels distribution systems. Scaleup of the spouted bed process and detailed examination of the Eagle-Picher process are recommended.

The Refuelable Zinc-Air Battery: Alternative Techniques for Zinc and Electrolyte Regeneration

1. Introduction and objectives

Introduction

Refuelable zinc/air batteries are "recharged" by an exchange of cell reaction products for fresh zinc and electrolyte. In electric vehicle applications, rapid refueling enables the vehicle to operate beyond the range limits imposed by its energy storage capability--allowing repeated use throughout the day interrupted by only short intervals for refueling. In fleet applications, expensive vehicles could be operated at a high capacity factor, allowing more rapid write-off of the initial vehicle investment. Lawrence Livermore National Laboratory (LLNL) has developed engineering prototype 6- and 12 cell batteries and demonstrated the capability for rapid refueling with 0.5-1-mm particles entrained in KOH electrolyte. Recently, a 6-cell zinc/air engineering prototype battery was successfully operated under sustained (5 hour) discharge conditions on an electric bus as part of a Zn/air-Lead/acid parallel hybrid [1]. (The bus was loaned by Santa Barbara Metropolitan Transit District). This battery established operating feasibility of a multicell stack using the patented self-feeding configuration [2].

This approach was inspired by- but differs from earlier work in refuelable and reconstructable zinc/air batteries: 100% of the zinc fuel introduced into this battery is consumed, and the battery can be brought from any state of discharge to 100% capacity without cost penalty or the removal of unconsumed metal. Moreover, if the zinc recovery could be accomplished using simple equipment operated at the fleet's home base, the industrial infrastructure (required by centralized fuel recovery schemes) could be avoided altogether. Applications of the self feeding cell are described elsewhere. [7,8]

This refuelable zinc/air battery requires external recovery of zinc and electrolyte from spent reaction products (zinc oxides and zincate). Following the demonstration of an engineering prototype multicell battery, the next step (pursued by this ILZRO-sponsored project) is to develop and demonstrate the essentials of a refueling cycle. In particular, we seek to learn how zinc particles fabricated by various techniques would feed into cells from filled hoppers, how the particles would settle within the cells, and how the morphology of the particles might impact cost and ease of refueling. Two routes to recycling were considered important to evaluate: the production of zinc particles in an electrowinning cell operated as a spouted bed and "seeded" with small particles; and a pelletized fuel fabricated by compaction of zinc fines electrowon as mossy or dendrite deposits. A third possibility, shot production by gas atomization or other technique, was also considered, although this approach would probably require industrial infrastructure and would not deliver the advantages of user/owner fuel recovery.

During the course of this study, three issues arose that are relevant to the scope of the ILZRO project. These issues concerned (1) possible shorting self-discharge during refueling because of particle bridging between adjacent anode hoppers; and (2) self-discharge of the zinc fuel during standby in the hot cell or during prolonged periods of non-use at ambient temperature; and (3) the cost of manufacturing of zinc shot for possible use as a fuel. These were addressed.

LLNL invented a process (patent pending) for the manufacture of zinc fuel pellets by compression of zinc fines within an electrolyte medium through use of a moving die [3] to form

1-mm pellets of 60% density. However, Eagle-Picher informed us of the existence of a proprietary process which yields compacted zinc plates of thickness 1 mm and comparable densities--by compaction of zinc fines (dry or wet) recovered from alkaline electrolysis of zincate solutions. The process is reportedly amenable to fleet-based use. The process is used in Eagle-Picher's manufacture of zinc electrodes for alkaline zinc batteries. This company offered samples of compacted disks, which we chopped into fuel pellets for test.

Finally, Noranda Technical Center (Quebec) furnished particles of coarse zinc powder, fabricated by the gas-atomization of molten zinc, for test in our cells as a potential fuel.

Objectives of this project

The objectives of this project are as follows:

(1) Conduct tests of a bipolar-cell configuration for recovery of zinc on inclined nickel electrodes, using natural electrolyte convection (anode bubble lift).

(2) Conduct tests of zinc electrowinning using a hydrogen-depolarized cathode.

(3) Modify the cells used in the on-vehicle tests of 6-cell battery by installing windows allowing visual observations of zinc particles in the discharge cell and overlying hopper.

(4) Test the discharge of cells using 0.75-1 mm pellets grown from 0.385 mm seeds in a fluidized bed (spouted bed configuration), supplied by University of California at Berkeley (Professor James Evans, PI).

(5) Discharge cells using pellets made of compacted zinc fines electrowon from alkaline electrolytes (product of Eagle-Picher, Inc.), comparing results with baseline cells using cut wire.

In addition these tasks, we list the following subsidiary objectives:

(6) Test particles of zinc manufactured by gas atomization of molten zinc (Noranda), under the same conditions as compacted zinc, fluidized bed product, and cut wire.

(7) Measure shorting currents (arising from electronic contact between adjacent hoppers through particles bridges) under conditions of refueling.

(8) Measure corrosion of zinc within battery electrolytes and in contact with battery hopper and current collector materials, at ambient and elevated temperatures typical of refueling.

(9) Determined energy-balance implications of zinc recovery using hydrogen-depolarized electrolysis as a route to recycle of battery reaction product.

(10) Estimate the cost of zinc shot from industry quotations, to provide a fuel cost baseline.

2. Zinc recovery by electrolysis at nickel electrodes

Background

Zinc is recoverable from alkaline solutions of zinc oxide and potassium zincate by electrolysis between nickel electrodes, according the reaction:

$$ZnO + H_2O + 2\,e^- = Zn + 2OH^- \qquad 2.1$$

$$2OH^- = \tfrac{1}{2}\,O_2 + H_2O + 2\,e^-$$

$$ZnO = Zn + \tfrac{1}{2}\,O_2 \qquad E_0^\circ = 1.619\ V$$

The evolution of oxygen occurs with low overpotential at the nickel anode, while zinc in dendrite or mossy morphology does not adhere well to a nickel or stainless steel substrate. A simple bipolar electrolysis cell was designed and constructed to allow deposition of particulate zinc on the upwards-facing surface of cold-worked, highly-oxidized nickel plates, while

downwards facing anodic surfaces sustains oxygen evolution. (Figure 2.1). This configuration confines oxygen gas bubbles near to the anode interface, where the gas buoyancy enhances intra-cell electrolyte convection as well as induces a net electrolyte transport through the cell. This configuration is potentially inexpensive and adapts well to the bipolar configuration. The bipolar array was constructed by sealing three 6 cm x 6 cm x 1 mm nickel plates in a slotted acrylic box (plate separation, 5 mm). Electrolyte was drawn into the array (by gas displacement) between long acrylic barriers which served to minimize shunt current losses between adjacent cells. Holes through the upper part of the box allowed return of the electrolyte to the tank.

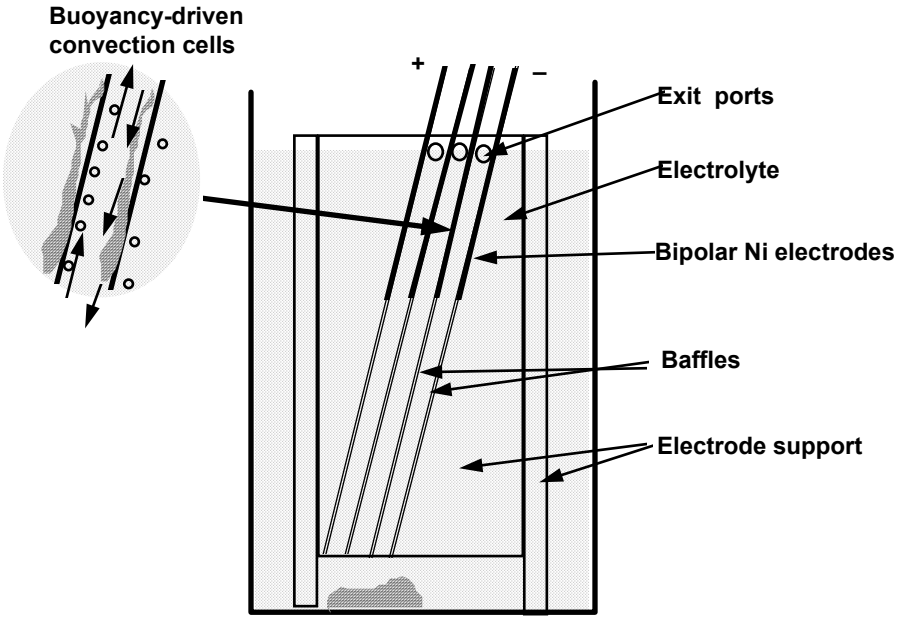

Figure 2.1 A bipolar array of cells was used in simple electrolytic recovery of zinc in the mossy morphology. The baffles extended 15 cm below the electrodes (not drawn to scale) to minimize shunt currents.

Two cells were operated at nearly constant voltage, while temperature and current were allowed to rise during electrolysis. The electrolyte contained 100 g-Zn/L dissolved in 12N KOH. The voltage of two cells (4.2 V) indicates an energy consumption of about 1.8 Wh/kg. (Figure 2.2). While the current density is quite low (<1 kA/m^2), the cell hardware is potentially inexpensive and therefore favors operation under low-rate, energy-efficient conditions. Because zinc deposition from alkaline electrolytes (as such) is well known, no further work was done beyond that required to introduce this configuration.

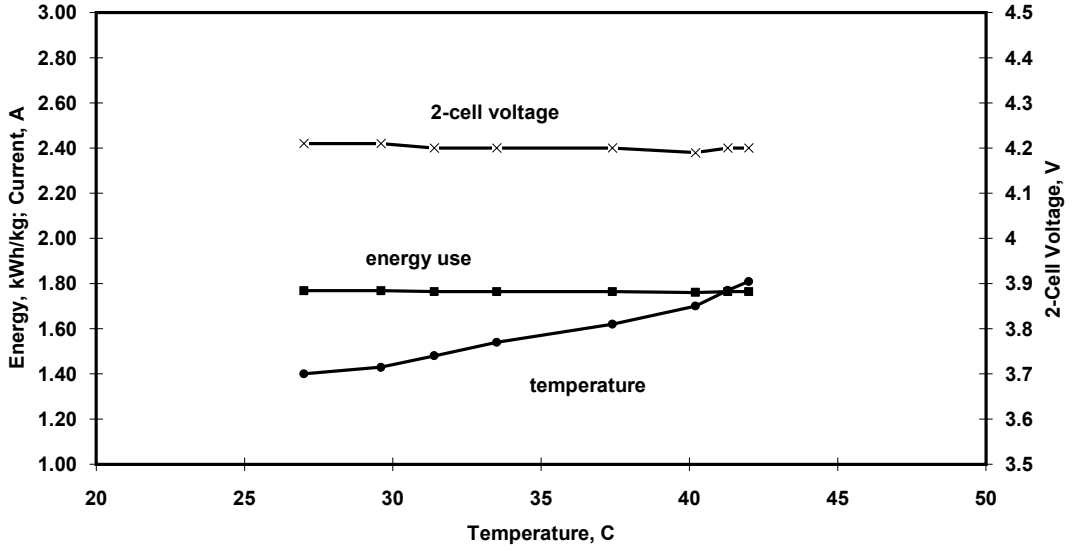

Figure 2.2 Zinc was electrodeposited in the mossy morphology on nickel electrode bipolar stack (two cells). Electrode area = 25 cm^2. The current varied directly with temperature, averaging 60 mA/cm^2.

3. Zinc recovery using a hydrogen-depolarized anode

Background

Zinc can be recovered from alkaline zincate solutions using a hydrogen depolarized anode. Hydrogen gas is passed over a porous carbon electrode catalyzed with 0.05-0.5 mg Pt/cm^2. The overall electrode reaction is

$$H_2 + ZnO = H_2O + Zn \qquad E_0° = 0.39\ V \qquad (3.1)$$

The standard electrochemical potential is the difference between the Zn/ZnO couple (1.619 V) and the H_2/O_2 couple (1.229 V). Hydrogen electrodes represent a highly developed technology and are used in nickel/hydrogen alkaline batteries in orbiting communications satellites, with operating lives of up to 72,00 hours. The hydrogen-assisted recovery of zinc by the above reaction was developed by New Jersey Zinc in the early 1980's under DoE contact (administrated by Drs. Albert Landgrebe and Stanley Ruby of DoE).

The hydrogen-assisted electrowinning of zinc is not used in primary electrowinning of zinc for reasons not relevant to this application. The industrial electrolysis uses acid solutions, from which zinc is electrowon at high rates as a dense deposit. Secondly, roasted zinc ores generally contain trace metals (Pb, As, etc.) which poison platinum catalysts required for the hydrogen oxidation. Neither of these issues is relevant to the recovery of zinc from alkaline solutions used in batteries free of these contaminants, where either particulate or porous deposits can be formed. The favorable energy balance ($E_0°$ = 0.39 V for hydrogen recovery vs. $E_0°$ = 1.619 V for

simple electrolysis) allows, in practice, a savings of 1.5 V. The significance of the reduction in energy use will be discussed in section 10.

Procedure

A hydrogen electrode was obtained from Eagle-Picher (Ni/H_2 No. 437) and sealed within an acrylic hydrogen flow chamber with provisions for current collection and electrode potential measurements. The active area was 25 cm^2. The counter electrode (cathode) was a plate of oxidized nickel supported at a distance of 6 mm from the anode such that electrolyte could flow between by natural convection. (Figure 3.1). Hydrogen gas at ambient pressure was generated by reaction of aluminum pellets in 12N KOH solution at 60 °C; the gas was collected in a funnel and passed through the anode chamber and thence through a tortuous-path exit tube. The electrolyte was produced by corrosion of zinc filings in hot 12 N KOH solutions, using nickel or stainless steel counter electrodes. The test solution contained approximately 100 g-Zn/liter (1.3 M).

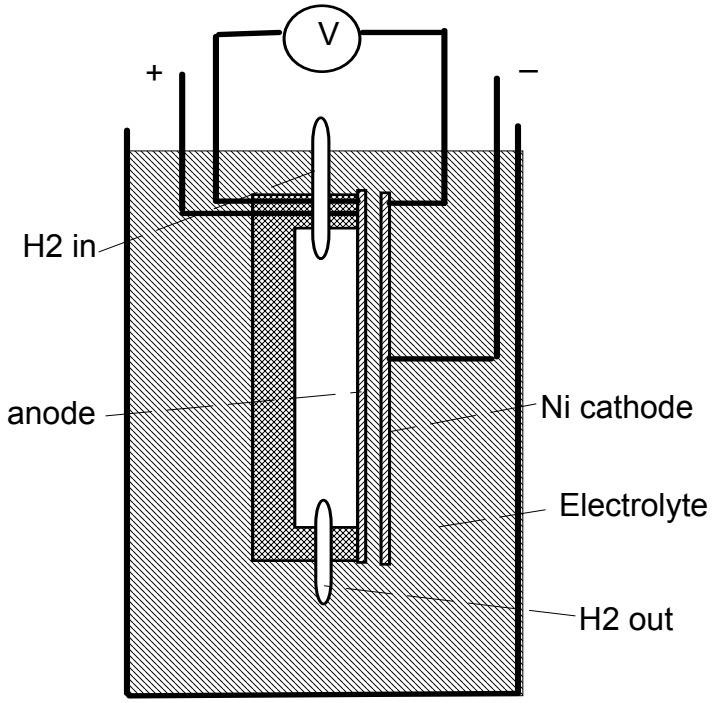

Figure 3.1 This experimental cell was used in experimentation with the recovery of mossy zinc with a hydrogen depolarized anode. The hydrogen gas slowly flows over the porous hydrogen electrode. The exit tube allows escape of water vapor entrained in the gas flow.

Results

The open circuit voltage of the cell was 0.45 V, indicating a significant corrosion potential possibly resulting from trace amounts of oxygen in electrolyte or gas; the theoretical O.C. voltage is 0.39 V. The polarization curve was linear and reflected the IR drop in the electrolyte. Raising the temperature from 28- to 40 °C and decreasing the inter-electrode gap to 3 mm reduced the resistance, producing a favorable set of operating conditions: E_{cell} = 0.6 V, i = 0.8 kA/m^2, T = 40 °C, and natural convection. Forced convection will be necessary in larger

installations. Having established a favorable operating point using existing electrode technologies, no further work was done with this process.

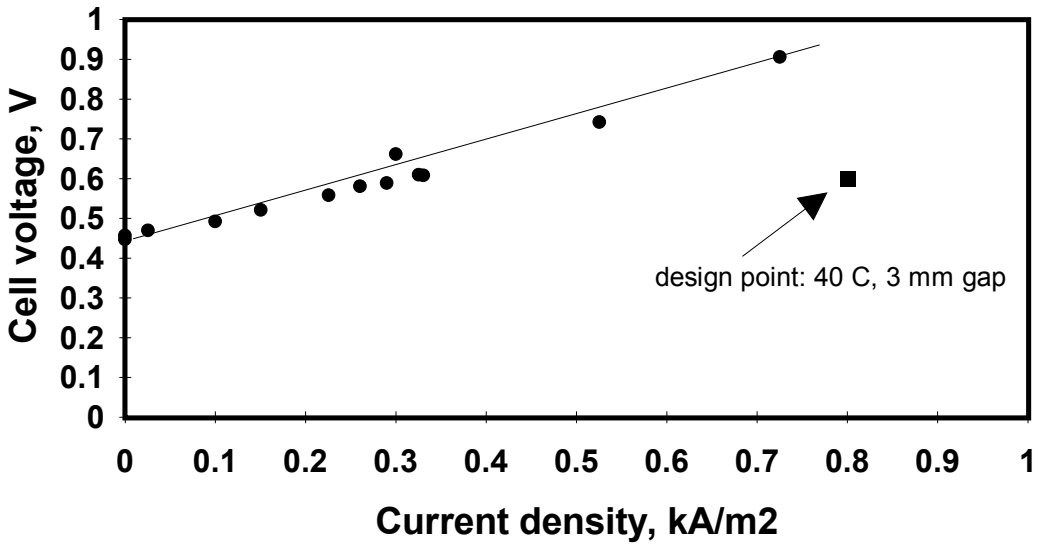

Figure 3.2. Polarization data are shown for hydrogen-depolarized reduction of potassium zincate solution at 28 °C and for electrode spacing of 6 mm. The hydrogen anode had an exposed area of 20 cm^2 (Eagle-Picher No. 437). Zinc was deposited on a 20 cm^2 nickel sheet electrode.

4. Experimental system used in cell discharge studies

A new experimental system was constructed for discharge tests using anode fuel produced by various techniques. The discharge cells were incorporated parts of the standard cell produced and tested earlier on an electric bus. [1] The bipolar transfer plates of these cells were modified by the addition of acrylic windows to allow direct observation of the transport of zinc particles. The windows were 1.2 cm wide and extended from the base of the cell to the top of the hopper. Two such windows were spaced symmetrically on the anode transfer plate.

These cells use porous gas diffusion electrodes catalyzed with Co-TMPP (Model AE-40, Eltech Research Company, Painesville OH). The AE-40 electrodes are constructed with a double layer of Exmet screen (Ag-plated Cu) which confines a hydrophobic mixture of carbons, catalysts and bonding materials. For convenience, we used silver-epoxy cement to affix the cathode current collector screen to the copper foil conductors soldered to the circuit board plates. This conductive epoxy bond does not show the low resistance of soldered or crimped connections and is not recommended for any applications requiring high power or efficiency. Nevertheless, the conductive epoxy allows non-destructive disassembly for examination and refurbishment of the frames. Since this bonding technique was used in the assembly of 3-and six cell stacks (the latter used in on-vehicle tests in February 1995), we have a basis for direct comparison with cut wire zinc pellets used earlier and reported elsewhere [1].

The experimental system is shown in Figure 4.1. The air was filtered through a soda lime filter (20 cm x 2.5 cm diameter) and regulated using a float meter and pin valve. Electrolyte flow was maintained at rates of 4 ml/s using a peristaltic pump. An average phase velocity of 0.5 cm/s was maintained in the cell. At a discharge rate of 2 kA/m^2, this flow rate confines the

maximum zincate concentration increase across the cell to 0.06 M, and the temperature increase to ~ 1°C. The electrolyte (1 L) was maintained at temperature in a controlled hot water bath. Thermocouples were provided to monitor temperatures at the entrance and exit of the cell, and within the hopper. An active load was used to control discharge rate. A power supply was operated at constant current (HP 30 A Power Supply), which produced an inverted (negative) voltage at the power terminals to compensate for the EMF of the cell. Discharge was sustained for prolonged periods at 20 or 35 A, with intermittent polarization sweeps between 10- and 50 A (0.4- 2 kA/m^2). The experimental operating conditions are given in Table 4.1

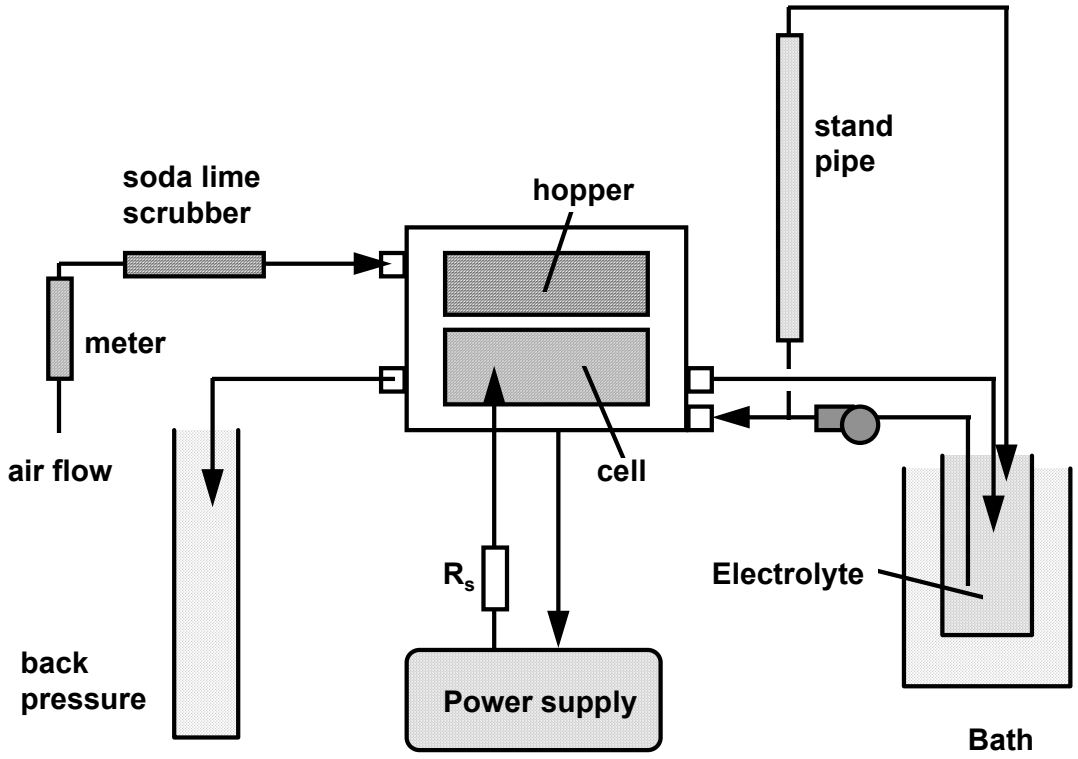

Figure 4.1. The experimental configuration depicted here was used in tests of alternative anode fuel morphologies and in self-discharge and shorting tests.

Table 4.1 Operating conditions used in the testing of self feeding cells.

Parameter	**Value**
Electrolyte (1L)	12 N KOH
Electrolyte flow rate	4 ml/s
Electrolyte temperature	50-60 °C
Air flow rate (4x stoichiometric)	60 ml/s
Current load (sustained)	20 A (0.8 kA/m^2)
Polarization range	10-50 A (0.4-2 kA/m^2)

5. Discharge using zinc spheres electrowon in a fluidized bed (UCB)

Experimental Procedure and Results

A constant current discharge experiment was conducted with 0.75-1.0 mm, prolate ellipsoidal particles grown from 0.385 mm diameter cut wire seed by Prof. James Evans (UCB) in a spouted bed. The purpose of the experiment was to determine whether particles produced by this method show the same facility for gravity-driven flow into and through the cell as cut wire. Microphotographs of the various test particles are shown in the Appendix, while further information may be found in the UCB report. The cell was assembled under normal procedures, but with the air electrode (Eltech AE 40) cemented to the cathode current collector with silver epoxy cement to allow facilitate assembly and disassembly. This high resistance bond lowers the voltage of the cell relative to that of the lower resistance solder, adversely effecting polarization, but should have no influence over the feed characteristics being studied. Since this silver epoxy cement was also used in the assembly of the 6-cell stack for on-vehicle tests, we decided to use this same method to allow direct comparisons in feed and polarization.

After the normal procedure for break in of a new air electrode (1 h under open circuit), the cell was discharged a controlled current (typically 25 A). The initial area of the cell was 0.025 m^2, but gradual dissolution of active zinc lowered the active area towards the end of the run. The electrolyte flow was somewhat lower than customary (2 ml/s vs. 4 ml/s).

The initial electrolyte volume was 1 liter. A small leak developed at the start of the experiment, which resulted in the loss of 95 ml of electrolyte into the air channel in the first hour; the leak was self-sealing, and the total electrolyte in the system was 850 ml upon close of the experiment, the difference (~55 ml) being lost by evaporation.

Figure 5.1 is a record of cell voltage, electrolyte temperature (inlet to cell), current (controlled), and accumulated discharge in units of Ah/liter (based on final volume of electrolyte). The cell area is constant, but the active area of the anode decreased due to dissolution of the anode without replenishment flow from the hopper (see below). Hence active cell area is not determined.

Figure 5.2 shows a polarization curve taken after 4 hours of discharge (roughly 50% discharge based on 250 Ah/liter limit). The curve is compared with the results obtained with the discharge of the 6-cell stack (average voltage of 6 cells in series) during the on-vehicle test [1], and is seen to be of comparable polarization. The curve is also compared with the best results under these operating conditions, obtained with a low-resistance cell (80 cm^2) assembled with soldered cathode leads soldered to the current collection lead and discharged using cut wire.

Upon conclusion of the test, the cell was disassembled and the electrodes examined. The spent electrode quickly (<10 minutes) separated into a clear supernatant fraction and a free-flowing precipitate, the boundary between the two being sharp.

Observations of feed

The feed was not uniform in several respects. For some reason, the particle bed failed to fall from the hopper into the cell, being restricted by the narrow 2.5 mm by 2 cm long channel between hopper and cell. While movement of the bed (i.e., feed) occurred *within* the cell, the bed adjacent to the windows did not appear to collapse uniformly over the course of the run. From the integrated current (141 Ah), one concludes that 173 g of zinc would have dissolved (or 38% of the initial bed).

Reasons for the failure to properly feed do not appear to be connected with the method of particle production, but rather with the small size of the interconnecting channels (designed for 0.75 mm particles) and possibly the high coefficient of friction of these porous particles. Several other operating factors might contribute to this lack of transfer: (1) No natural vibrations were imparted to the cell, such as in the on-vehicle test or with the centrifugal flow pumps used in earlier laboratory tests. (2) The particles were larger than any previously tested in this particular cell (i.e., 0.75-1 mm vs. 0.50- 0.75 mm), which tends to slow the collapse of the bed because of the enhanced bridging in the 3 mm gap. (3) The channel between the bed and the hopper was narrower than ideal for this particle size, and was further reduced to 2.5 mm by a coating of silicone cement, which increased friction. None of these effects rule out the use of particles grown in fluidized or spouted beds, as each problem can be solved by enlarging the opening of the entry to the cell and the width of the channel connecting hopper to cell. The silicon cement blockage was removed from subsequent tests, increasing channel width to 3.0 mm.

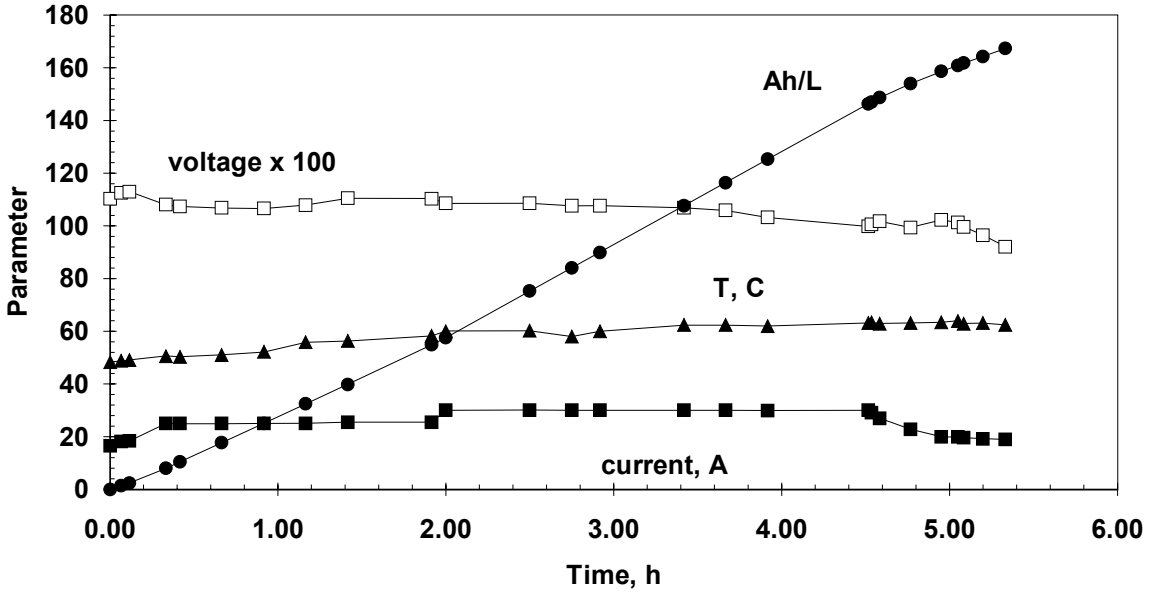

Figure 5.1. Discharge record for cell filled with 500 g of 1 mm particles grown in a spouted bed (UCB). Shown are cell voltage (x100), cell electrolyte temperature (°C), cell current (A), and accumulated discharge (units, Ah/L).

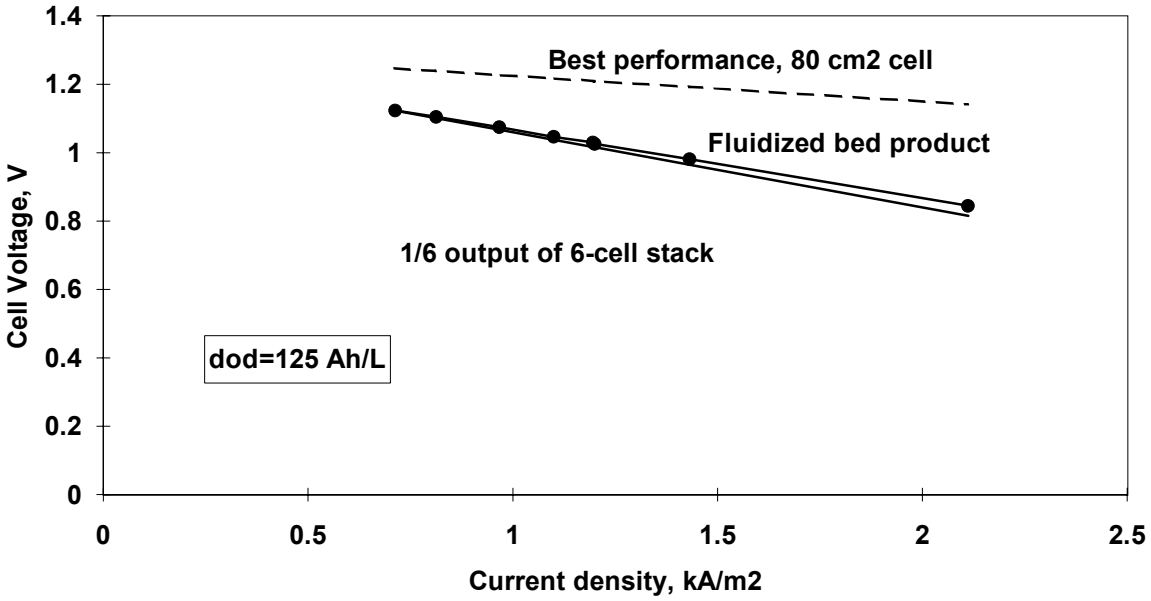

Figure 5.2. Polarization curves at ~50% depth of discharge (125 Ah/liter) for 0.75-1.0 mm particles produced in a spouted bed (data points), compared with corresponding average-cell results from the 6-cell stack test on the vehicle (solid line) [1]. Also compared are results obtained under similar operating conditions, but with solder connection to the air cathode screen (as opposed to the silver epoxy connections made in this test and for the cell stack) and with a total cathode area of 80 cm^2 (broken line).

6. Discharge using shot formed by gas atomization (Noranda)

Procedure and Results

Noranda Technology Center (Quebec) supplied samples of shot and gas atomized coarse powder. The shot was too large for our test cells, which could not be readily modified for this size. The coarse powder was sieved and the fraction having the size 0.6-0.83 mm was tested in the cells under the same conditions as before (Section 5). This powder consisted typically of spindle-shaped particles with polished surfaces and rounded ends. Length/width ratios were in the range of 4-8.

During discharge, the hopper fed continuously into the cell (Figure 6.1) , similarly to the cut wire and coarse powder tested earlier. The displacement was somewhat less than expected based on an assumed packing density of 50% and galvanic dissolution of the zinc. The packing density could conceivably be greater than 50% because of the long aspect ratio of the coarse powder and consequent stacking. Despite the irregular shapes of these particles, the bed showed the greatest fluidity of the samples tested in this study and conformed most closely to the behavior of the cut wire used earlier for comparison.

The discharge record (Figure 6.2) and polarization (Figure 6.3) were similar to that of the fluidized bed product, but with somewhat improved polarization. This polarization increased strongly with Ah/L loading of the electrolyte (Figure 6.4), in contrast with either spouted bed particles or compacted fines. The cause of this greater polarization was not ascertained, but

could result from a progressive increase in cell hydraulic resistance as the particles settled into the cell and stacked as wires (i.e., with lower void fraction) rather than as roughly spherical beads.

Conclusions

Gas atomized coarse powder appeared to flow steadily into the cell, despite irregular shapes. The plot of level of hopper against Ah discharge showed a lower slope than expected for 50% packing density but roughly that expected for 60% density. It would be desirable to test a more rounded shot of dimensions ~ 1 mm made by a gas-atomized or free-fall technique, as this fabrication technique is potentially low cost.

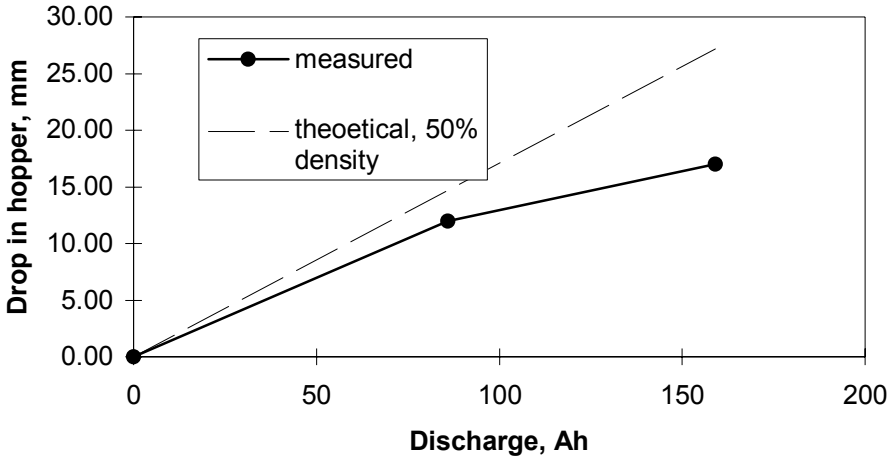

Figure 6.1 Fall in zinc level in the hopper during discharge, compared with that calculated for a 50% void fraction. The anode consisted of gas-atomized zinc powder (Noranda).

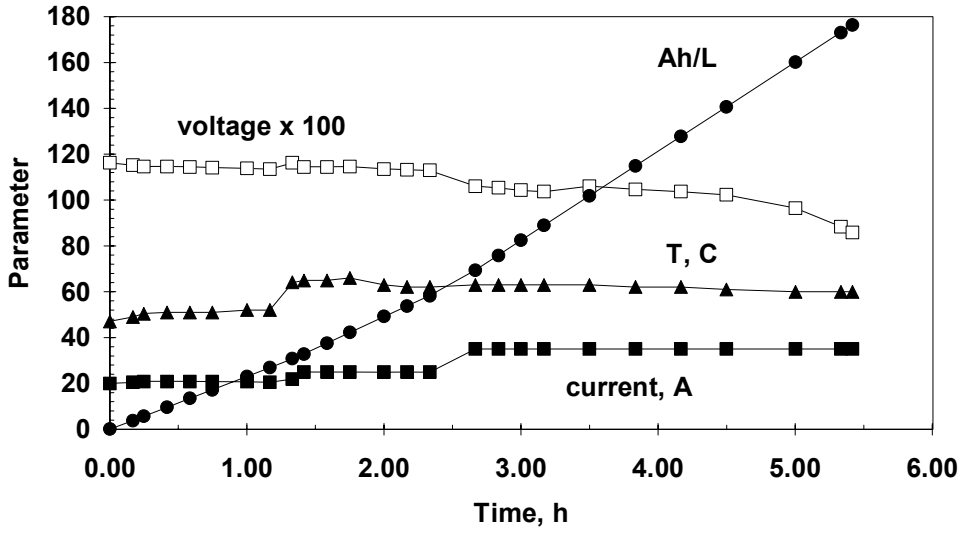

Figure 6.2 Time records of discharge are shown: voltage x 100; electrolyte loading in Ah/L; temperature; and current. The anode consisted of gas-atomized zinc particles (Noranda).

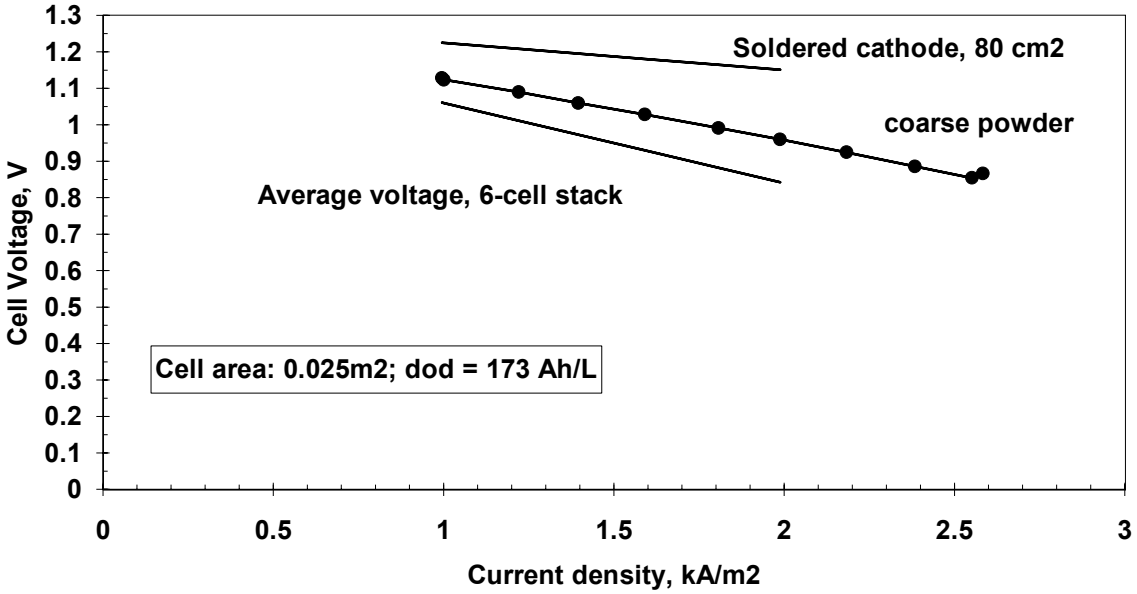

Figure 6.3. Cell polarization at 173 Ah/L (end of run), compared with 6-cell stack and soldered cell results. Data points: discharge of zinc particles (Noranda); "dod" means "depth of discharge."

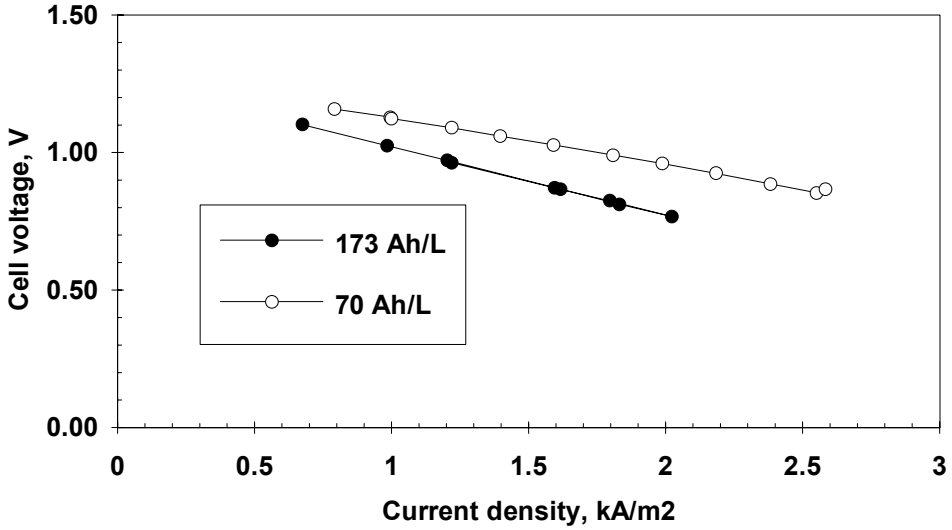

Figure 6.4 Polarization curves at 70- and 173 Ah/L discharge for gas-atomized zinc particles (Noranda).

7. Discharge using pellets produced from compacted fines (Eagle-Picher)

Background

In 1994, LLNL experimented with pin-and-die presses to compact zinc particles into 1 mm x 1 mm right cylinders of 60% density. Both die and pin were made of stainless steel, with sufficient clearance (0.005 inches) to allow removal of the excess liquid. An insufficient number of pellets were produced to allow testing in a cell: 0.5 kWh would require 150,000 pellets of these dimensions and 60% density. The particles produced remained intact when subjected to agitation in electrolyte greater than that found in normal transport.

Eagle-Picher, Inc. (Joplin MO) furnished us with samples of compacted zinc disks 7.6 cm diameter by 1 mm thick and 60% density. The plates were produced by a technique used in the manufacture of electrodes for alkaline Zn batteries, and entails the wet or dry compaction of high purity electrolytic fines without the use of a binding agent. A hydraulic press was used in the compaction of these samples. The industry representative reported that the preparation and compaction technique (which is proprietary) is compatible with a continuous rolling operation [5]. Consequently, the technique could be potentially down-scaled for dedicated fleet recovery operations.

Procedure and results

The plate was chopped into particles using stainless steel blades, and then. Two grades were produced: 0.6-0.83 mm cross sectional dimension by 1 mm thick; and 0.83-1.2 mm cross sectional dimension by 1 mm thick. Approximately 20% was below 0.6 mm and was discarded, while 20% fell into the range 0.6-0.83 mm; the balance was of the larger dimensions, 0.83-1.2 mm. All particles were flat and parallel on two side, and 1 mm thick.

Five hundred grams of compressed zinc pellets were loaded into the cell with a previously unused air electrode and separator. Of this zinc, approximately 120 g of the smaller dimension were loaded first, and completely filled the active part of the cell. The fraction with the larger dimensions (380 g 0.83-1.2 mm) was loaded into the hopper.

The procedure of air electrode break-in (45 minutes at a low current of 12 A) was followed here. Figure 7.1 shows the time record of a discharge experiment lasting 8 hours and resulting in a 250 Ah/L loading of the electrolyte. The smaller fraction settled continuously within the cells. However, the larger grade of zinc in the hopper did not continuously feed into the cells. At 3 hours, the smaller grade of zinc in the cells was substantially consumed, causing the potential to drop. It was necessary to probe the hopper with a wire to introduce the larger pellets of zinc (0.83-1.2 mm) into the cell at about 3-5 hours after start of discharge. A polarization curve, taken at 160 Ah/L, showed discharge characteristics favorable to the average of the 6 cell stack using cut wire (Fgiure 7.2).

A comparison of polarization curves at 47- and 160 Ah/L in Figure 3 showed little effect of polarization on depth of discharge. In fact, the efficiency of discharge appeared to improve slightly from 47- to 160 Ah/L. Precipitation of solids in the cell is observed nearly from the start of discharge, as a cloudy phase in the electrolyte. The weak dependence of polarization on Ah/L loading of the electrolyte can be attributed to the low solid fraction of zinc oxides in the electrolyte. (See below).

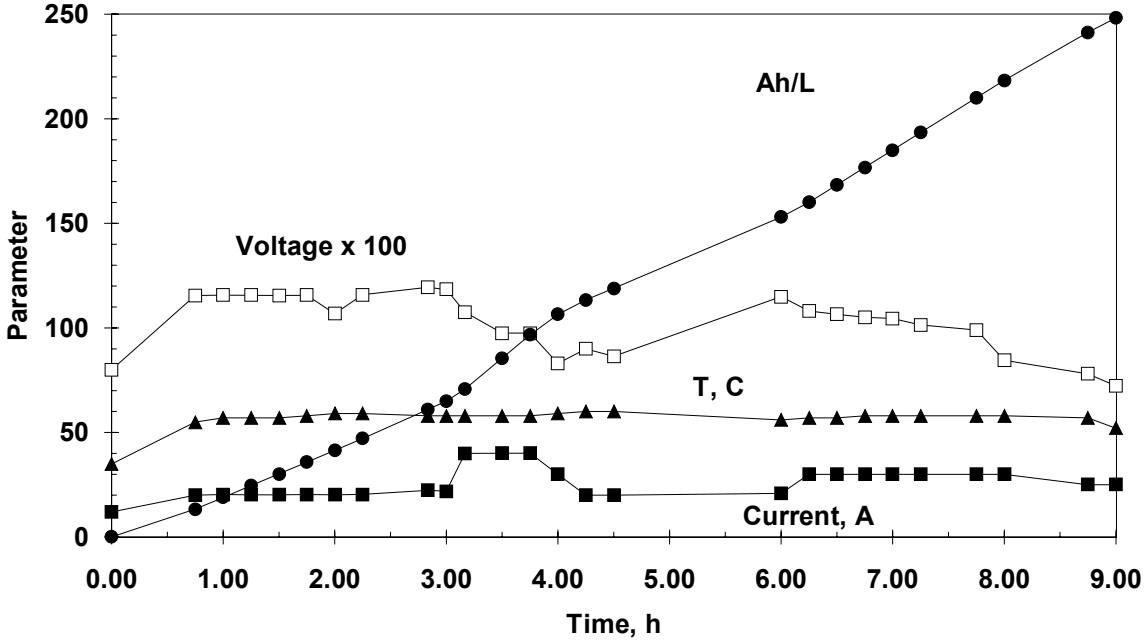

Figure 7.1. Time-record of discharge of cell using particles of compacted zinc fines (Eagle Picher). Only particles of size 0.6-83 mm fed into the cells; larger particles (0.83-1.2 mm) (after 5 hr) required stirring of the hopper with a wire probe.

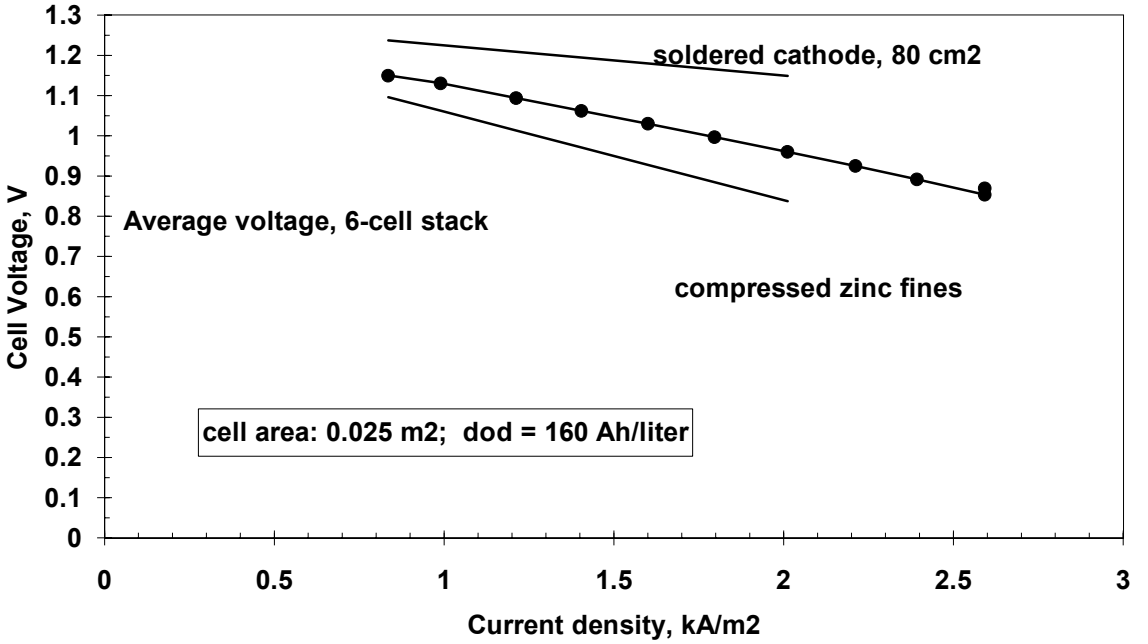

Figure 7.2 Polarization of the zinc/air cell filled with 0.83-1.2 mm particles of compressed zinc (Eagle Picher) (data points). The lower solid line is for the 6-cell reference; the upper curve is for small cells with soldered current collectors.

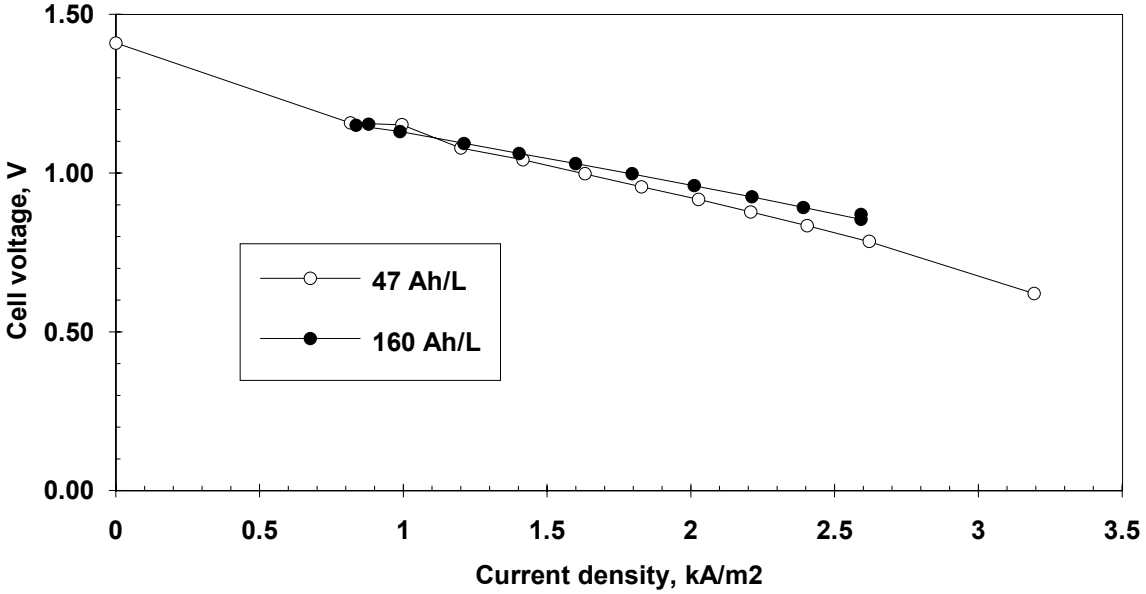

Figure 7.3. Polarization curves at two stages of discharge, 47- and 160 Ah/L, show little change in efficiency. The zinc pellets were chopped from compressed zinc plate (Eagle-Picher).

Conclusion

Tests with compressed zinc particles (60% density) showed continuous feed and polarization characteristics only for the smaller of the two sizes tested: 0.6-0.83 mm cross section by 1 mm thick. Large particles (0.83-1.2 mm) did not spontaneously feed into the cells. Polarization curves at 47- and 160 Ah/L loading (depths of discharge) were similar, indicating that the accumulation of solid particles of discharge products did not significantly alter the conductivity of the electrolyte. Assuming all the discharge products at 160 Ah/L were solid ZnO (zincite), the solids would occlude only 4.4% of the electrolyte volume, and thus have a minimal effect on electrical resistance.

8. Self-discharge of an oxygen-depleted cell during refueling

Background

During the refueling operation, cells are refilled by a hydraulic transfer of zinc fuel pellets entrained in zinc-depleted electrolyte. During this operation, it might be expected that zinc particles should bridge adjacent cells, effecting a short circuit between anode and cathode current collectors. To prevent catastrophic self-discharge, the flow of air into the battery must be shut off at the exit, and the resident oxygen remaining in the cells is consumed by discharge through a load (e.g., a secondary battery for vehicle startup or auxiliaries). Since the ambient volume of air in the cell and connecting tubes is very low (<100 ml/cell), the energy consumed

by oxygen depletion is small (<310 A-s/cell and amounts to < 0.13 Wh/cell. The hopper initially contains 500 Wh; < 0.3 ppt of the energy capacity of the filled hopper.

An intuitively more important question concerns the discharge of a zinc/water cell during shorting during recharge under oxygen depleted conditions, according to:

$$Zn + H_20 = ZnO + H_2 \quad (E^o = 0.37\ V) \qquad (8.1)$$

To determine worst-case rates of discharge, we need to know both a polarization curve for a Co-TMPP-catalyzed zinc/water cell (at operating temperature) and a "load line" derived from the worst-case (lowest) resistance of the shunted cells. The intersection gives the rate of reaction (8.1) as a current density. This analysis is developed here, and will be compared with actual experiments with shorted single cells using the Noranda gas-atomized zinc powder and the Eagle-Picher compacted pellets.

Procedure and results

The resistivity of a zinc particle bed (0.7 mm cut wire particles in ZnO-saturated 12 N KOH electrolyte) was measured in a U-shaped Pyrex conductivity cell of conduction length 30 cm and of internal diameter 1.78 cm; the cell constant is thus 0.083 cm^{-1}. Resistance was measured using the four-wire technique: currents were applied with a power supply using stainless steel cylinder conductor probes (0.63 cm diameter), which also were used to compress the bed. The potential-measuring probes were stainless steel (0.3 cm) touching the bed. For samples left overnight at ambient temperature, the resistance was measured to be 0.49 Ω. After passage of large amounts of current (10 A) for periods of several minutes, with vigorous shaking and compacting of the bed, the resistance fell to a minimum 0.25 Ω. Therefore, we bound the resistivity of the bed as 0.02-0.04 Ω-cm. (Figure 8.1) This resistance is electronic in nature, and is greatly exceeded by the ionic resistance.

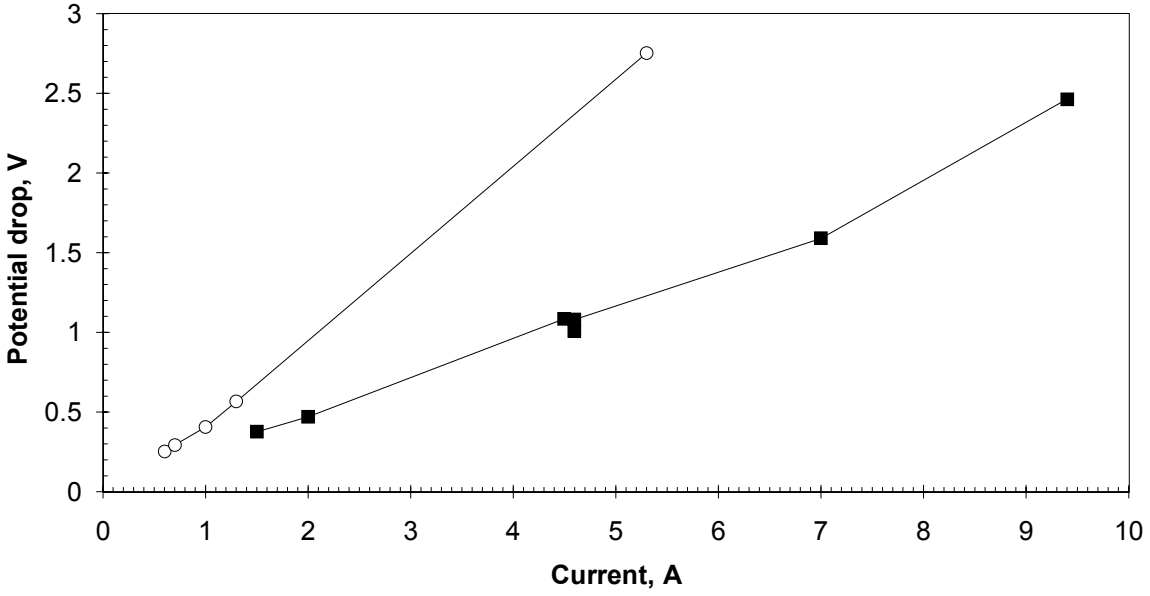

Figure 8.1. Resistance as function of current for packed beds of 0.75 mm (0.030 inch) cut wire in ZnO saturated 12 N KOH at ambient temperature, measured in a 4-wire conductivity cell of

0.083 cm^{-1} cell constant. Open data points are initial resistance (after 18 hours standby in cell); closed data points are lowest resistance after passage of 10 A and mechanical compacting. T = 24 °C.

Load-line for assembled cell stacks. Because of the substantial resistance of the bed, it is necessary to determine the total resistance of various components in the cell. This is done be summing the cell constants in the standard experimental cells, as given Table 8.1. For two adjacent cells shorted by a bridge of zinc 0.5 cm deep, the cell constant is 7.16 cm^{-1} and the total resistance is in the range of 0.14 - 0.29 Ω.

Table 8.1. Geometric constants for cell parts

Component	**L/Area (cm^{-1})**	**Contribution (%)**
Cell (1/2 depth)	1.6	44.5
Traces (hopper to cell)	0.37	10.3
Hopper (filled)	0.41	11.5
Fill tubes and drop slots (per cell)	1.2	33.5
Total	3.58	100%
2 X total (for two adjacent cells)	7.16	

Measured polarization curves for Zn/H_2O cells. Figure 8.2 shows a polarization curves for the cell, Zn/H_2O/Carbon CoTMPP at ~ 49 °C and at 58 °C, using, respectively, zinc coarse powder (Noranda) (0.6-0.83 mm) and porous zinc pellets (Eagle-Picher, Inc.) (0.6-1.2 mm). The curve was obtained by shutting off the oxygen flow to the cell under resistive load, and allowing potentials to drop from Zn/O_2 levels (1.2-1.4 V) to Zn/H_2O levels (E_o = 0.37 V). By shorting the cell through a range of low resistance wires (0.2-1 ohm), we constructed the reported polarization curve of Figure 8.2. The solid data points are for a cell loaded with Noranda air-blown shot; the open data points were taken on a separate experiment at 58 °C, using 60%-dense compressed zinc particles (0.6-0.83 mm) (Eagle Picher). Superimposed on this chart are load lines (normalized to 250 cm^2 cell size) for resistance of the bed (35-70 ohm-cm^2). The intersection gives a self-discharge current density in the range of 3-5 mA/cm^2. This is a scale factor.

In a shorting experiment, a 3 mm stainless steel probe was pressed into the hopper (open data points) to a depth of 2 cm, and the maximum shorting current was measured between the probe and the cathode current collector of the same cell. A current of 2.5 A was measured at a voltage of 0.195 V. When this value (10 mA/cm^2) was reduced by the increased resistance as calculated for the beds in *two* adjacent hoppers and the resistance intervening bridge between the cells (Table 8.1), the broken load line was constructed giving a worst-case shorting self-discharge current density of 3.3 mA/cm^2. This value, for compressed zinc particles (Eagle-Picher) at 58 °C is within the range calculated for the more conductive cut wire or powder. We can conclude that the worst-case shorting current during filling of an oxygen-depleted cell will be in the range of 3-5 mA/cm^2, or about 1 A for a 250 cm^2 cell.

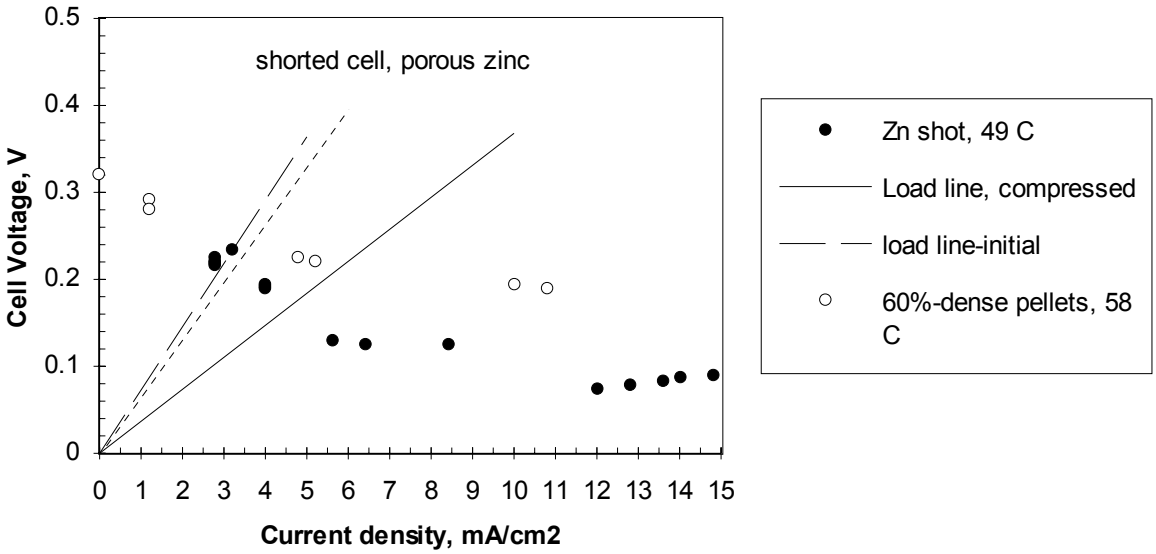

Figure 8.2 Polarization curves for zinc/water cells containing packed particle beds. Open data points, 0.6 mm compressed zinc pellets (60% dense; Eagle Picher) at T = 58 °C. Closed data points, gas-atomized coarse zinc powder, 0.6-0.83 mm (Noranda) at T = 49 °C. The dotted line is based on experiments with Eagle-Picher compressed zinc pellets (T = 58 °C) for shorting between cathode and hopper and projected for the case of shorting between two adjacent cells (two hoppers).

Implications for energy balance of zinc/air cells

For an array of 180 cells, refilled in 10 minutes, the shorted cell discharge will occur for an average of 4.5 minutes. (1 minute startup; 9 minutes fill). The capacity loss will be 13.5 Ah, or < 0.02% of the capacity of a typical 90 kWh (72 kAh) battery. The heat dissipation will be 0.2 W/cell (36 W total). The hydrogen evolution rate will be 0.16 ml/s per cell, or a total of 5.6 L for the assembled battery for the 10 minute refueling.

In conclusion, the shorting that should occur during zinc refilling of an oxygen-depleted cell results in a negligible energy loss (<0.02 %), negligible heat dissipation, and a volume of hydrogen evolution which may be readily dissipated by the design air flow of the system. The amount of self discharge can be reduced by increasing length (resistance) of the drop slots connecting the fill tubes to the hopper, should this be desired.

In earlier work, we have left a zinc-filled 3-cell stack at open circuit exposed to ambient hydrogen atmosphere for 12 days, without suffering a measurable deterioration of cell polarization upon subsequent discharge (as Zn/air). This suggests that the cobalt-complex catalyst is not substantially altered at hydrogen reduction potentials in alkaline electrolyte over that time period. (Under standby conditions, the cathode voltage can be controlled at any potential near to 0.4-0.5 V vs. Zn simply by allowing a trickle discharge). Further work is warranted in the area of Co -TMPP catalyst stability under various standby scenarios.

9. Zinc corrosion during refueling and standby

Background

Zinc may be consumed during refueling or on standby by the corrosion of zinc in contact with the metal anode current collector in the electrolyte-flooded zinc particle bed. This corrosion does not involve the air electrode, as air flow is shut off during refueling and on standby. (If oxygen is present, a small quantity of hydrogen peroxide can form, diffuse into the anode bed, and promote oxidation of the zinc. This reaction is slow and is not relevant to the use of this battery.)

During long periods on standby, the zinc anode approaches ambient temperatures. (The thermal time constant for our 6-cell battery is 14 hours). During refueling after sustained discharge, the bed will be at a temperature of about 60 °C. Appropriately, we measured the self corrosion of zinc in contact with various metals and a saturated (~ 1N KZnOOH) electrolyte at both ambient and elevated temperatures, in order to estimate the effect of corrosion on capacity loss and efficiency.

Procedure

Graduated glass pipettes (10 ml capacity) were sealed at the exit end then completely filled with zincate-saturated electrolyte, 20 g zinc particles (0.75 mm) and samples of metal foils or wires (area = 10 cm^2) in close contact with the zinc. The zinc electrode (consisting of 0.75 mm right cylinders) has an aggregate surface area of 225 cm^2. Hence the anode/cathode area ratio for these tests is 22.5. The electrolyte used was that from the discharge of a zinc/air cell using zinc particles grown in a fluidized bed, having a zinc loading of 125 Ah/liter. The samples of current collector metal included Exmet (Delker, Inc. product 4 Cu 7-100 tin plated and flattened); strips of solder (Pb-0.5 Sn; and Sn-0.05 Sb); and tin and copper foils. The wide end of each pipette was then plugged with glass wool (to allow slow exchange of electrolyte) and up-ended in a vessel filled with the same electrolyte. Gas volumes collecting in the pipettes were then recorded at various times over a period of 5 days.

From the measured corrosion current in these cells, we bracketed the estimate of corrosion in battery cells of any size by predicting total cell corrosion rates for two extreme conditions: (1) The corrosion is controlled by the polarization of the anode (in which case the corrosion rate is proportional to aggregate zinc area and therefore to zinc mass; and (2) the corrosion rate is controlled by the current collector metal kinetics, in which case corrosion is proportional to current collector area. The larger of the two predicted values will be taken as the upper bound to self-discharge of the zinc/air cell under standby conditions.

Table 9.1 gives corrosion data for ambient temperatures (over a 5 day period) as well as for 57 °C (over 3 hours). Corrosion current (in mA) is calculated from Faradays Law and the Ideal Gas Law (with Dalton's Law correction for the vapor pressure of water). A corrosion current density is then calculated based on the aggregate area of the zinc particles (225 cm^2) and the current collectors (5- or 10 cm^2).

Finally the total corrosion currents are calculated for the single cell having total anode mass of 100 g (anode limited case); and also for the total current collector area of 325 cm^2 based on the area of the cell's screen and transfer plate. These last two values are given in the last two columns of Table 9.1

Table 9.1 Corrosion of 20 g zinc (225 cm^2) in simulated cells at ambient and elevated temperatures

Collector	Area	T	Time	Vol. H_2	Current	Anode CD	Cathode CD	Zn-Lim	CC-Lim
	cm^2	°C	h	ml	mA	μA/cm2	μA/cm2	mA	mA
Low Temperature									
none: control	0	22	115	1.2	0.19	0.85	--	0.96	--
Sn-0.05 Sb	10	22	95	6.9	1.34	5.9	133	6.7	43
Sn-0.50 Pb	10	22	115	2.2	0.35	1.6	35	1.8	11
Sn (99.88%)	10	22	115	2.0	0.32	1.4	32	1.6	10
Sn plated Cu exmet	5	22	115	0.9	0.14	0.64	29	0.72	9.4
Cu	9	22	115	1.4	0.22	1.00	25	1.1	8.1
High Temperature									
none: control	0	57	3	0.5	2.6	11	--	13	--
Sn-0.50 Pb	10	57	3	2.4	12.3	55	1230	61	399
Sn (99.88%)	10	57	3	0.6	3.1	14	307	15	100
Sn plated Cu exmet	5	57	3	0.1	0.51	2.3	102	2.6	33
Cu	9	57	3	0.4	2.05	9.1	227	10	74

Conclusions

In all cases, the current collector appears to be controlling hydrogen evolution, the discharge current on the anode being comparatively small. In the control case (no current collector metal in contact with the zinc) the anode corrosion current density was insignificant (0.9 μA/cm^2 at 24 °C; 11 μA/cm^2 at 57 °C). When corrosion was scaled using the current collector area, Sn-0.05 Sb solder was found to be the most corrosive system, while tin-plated copper Exmet gave total corrosion values of only 9.4 mA and <33 mA for 24- and 57 °C respectively.

At ambient temperature (24 °C), the corrosion loss of zinc for a 500 Wh cell under prolonged standby is negligible: The loss amounts to <7 Ah/month, or 1.75% of total cell capacity per month.

At high temperature (57 °C), the corrosion loss is also negligible: if such high temperatures are maintained overnight (in for example a well-insulated cell), then the total energy loss from corrosion (12 hours) is 0.4 Ah per cell, or 0.08% of total cell energy capacity (500 Ah).

10. Energy balance of zinc recovery using hydrogen gas; cost of shot

Energy Balance

Hydrogen gas can be used in the electrolytic recovery of zinc from alkaline zincate solutions in a centralized industrial recovery plant. This is a long-range option not suggested for fleet-based operations. Still, the energy efficiency is important and judging long-term viability of zinc as a transportation fuel, under conditions where global energy balance might be important.

Table 10.1 gives the energy inputs required to convert (as an example) natural gas to hydrogen for subsequent use in hydrogen-anode electrolysis. For each kilogram of zinc produced by this method, 4.357 MJ of natural gas (NG) are consumed through electricity production together with 6.726 MJ of natural gas through hydrogen production at 62% efficiency. The ratio of the electricity output of the battery to the sum of the natural gas inputs (3.75/11.083 = 0.34) is the primary energy utilization, measured at the battery terminals (Table 10.2). This utilization is similar to that of hydrogen/oxygen fuel cells, but the zinc-air system is roughly an order of magnitude lower in initial cost [1]. At the same time, the use of zinc as a vector for hydrogen obviates issues storage and handling of hydrogen or on-board reforming of fuels.

The comparative energy flows for zinc/air (electrolytic recovery), zinc/air (hydrogen anode recovery) and hydrogen use in fuel cells is shown in Figure 10.1.

Table 10.1 Primary energy used in production of zinc through hydrogen intermediate, and energy yield from battery terminals.

Energy	**Basis**	**Incremental MJ/kg-Zn**	**Sum MJ/kg-Zn**
*Zinc production from NG**			
Zn recovery electricity at cell	Empirical (Eagle-Picher anode)	1.614	
Electricity at plant	95% rectification/distribution	1.699	
Total electricity, reduced to NG basis	39% base load: (1.699/0.39)	4.357	4.357
H_2 use	1 mole/mole; HHV	4.372	
H_2 reduced to NG	62% efficiency	6.726	6.726
Total Primary energy input			**11.083**
Zinc Battery discharge			
cell voltage @ 1 kA/m2	1.29 V empirical; 98% net coulomb efficiency	3.750	**3.750**

*NG = natural gas.

Table 10.2 Total energy conversion efficiency (natural gas to battery output electricity) and electrical energy multiplication.

Efficiency factor	**Basis**	**Efficiency**
Total conversion efficiency	3.75 MJ/kg-Zn output/ 11.083 MJ/kg-Zn input	**0.34**
Total electrical efficiency	Electrical output/ electrical input	**2.37**

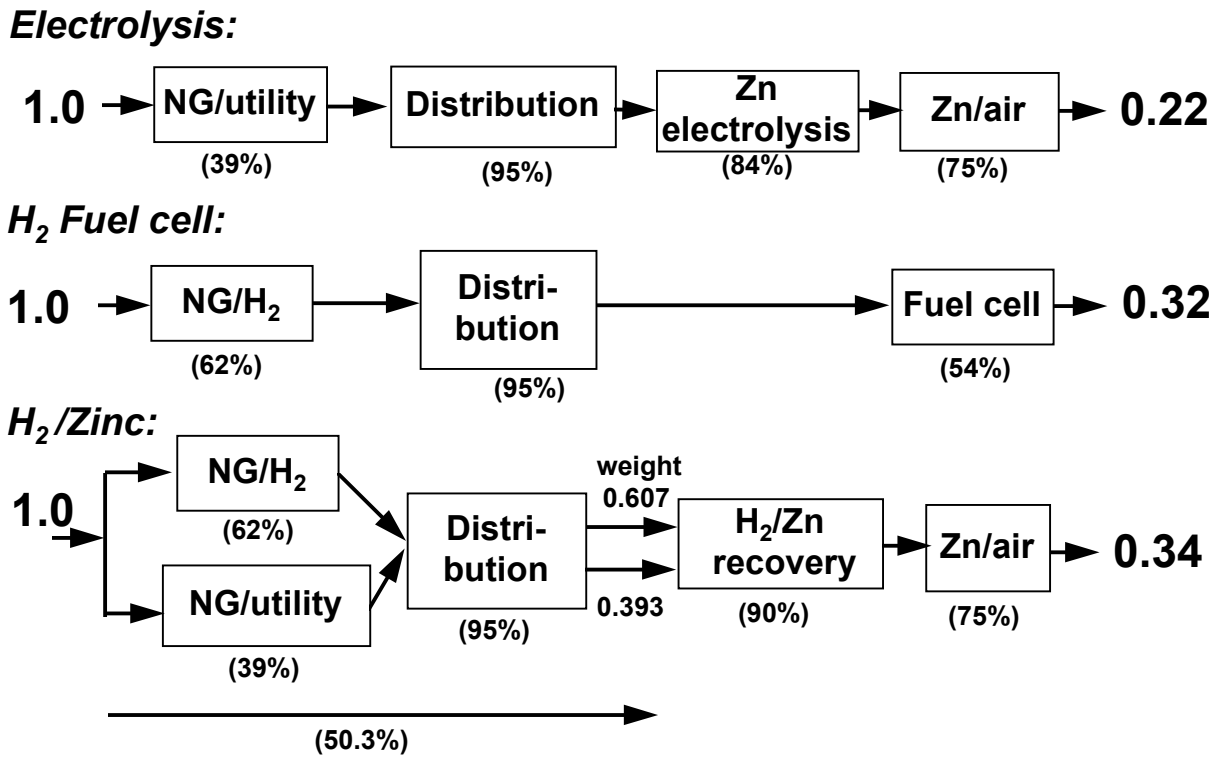

Figure 10.1 Energy flow chart for zinc/air refuelable batteries with conventional electrolytic recovery, fuel cells using hydrogen produced from 1 unit of natural gas energy, and zinc/air refuelable batteries using zinc recovered through hydrogen-anode electrolysis. Numbers on the right of the diagram (0.22, 0.32, 0.34) give the fraction of the HHV of the natural gas input which is converted to battery electrical energy output.

Cost of Zinc Shot

We are awaiting estimates from Noranda concerning the cost of gas-atomized coarse zinc powder and shot.

A usable fuel could be made by electrowinning rough slabs of zinc from the battery product, melting, and dropping back into the zinc-depleted electrolyte. Huron Valley Steel quoted the incremental cost of producing zinc shot from super purity zinc ingot to be 1.5-3 ¢/lb over the base price of super purity zinc ($0.48/lb on London Metals Exchange and $0.52/lb on American Spot Market, March 1996) [6] . Since the energy yield of the zinc under low current density discharge anticipated for hybrid vehicle applications is about 1 kWh/kg, the cost of fuel fabrication by melting and shot freezing is about 3.3-6.6 ¢/kWh. Any technique for centralized, large-scale production of zinc fuel pellets should be compared with this baseline. Indeed, this is a useful starting point for comparison of various zinc/air approaches.

The energy cost of shot production (considering the heat of fusion of zinc [96 J/g] and the poor efficiencies of heat recovery from such processes) is on the order of 2% of the gross electrical energy yield of zinc in the battery.

11. Conclusions

Conclusions of this work are as follows.

1. *Zinc electrolysis.* In small scale tests, zinc was recovered in the mossy morphology in a bipolar array of treated nickel plates, inclined to allow oxygen evolution to drive convection cycles in the inter-electrode gap. Since this configuration is not expensive (being constructed of nickel-plated copper foil and obviating external current collectors), it may be operated at a low current density and high energy efficiency of 1.80 kWh/kg-Zn, or ~90% charge efficiency.

2. *Hydrogen-anode zinc electrolysis.* Hydrogen gas can be used to recover zinc at 0.6 V in a 3 mm cell at 40 °C. This is about 1.5 V lower than in simple electrolysis with oxygen evolution.

3. *Feed characteristics.* None of the three routes to zinc fuel pellets (electrochemically formed, melt-formed and compressed zinc fines) can be ruled out on the basis of performance in the self-feeding cells, despite different results. The failure of the fluidized bed product to feed from hopper into cell may be attributed to the small size of the interconnecting channel, (designed for 0.75 mm particles); this can be overcome simply by decreasing the size of the particle relative to the width of the connecting channel, or by increased gap. The 0.83-1.2 mm particles produced by chopping compressed zinc disks (Eagle-Picher) were clearly too large for the existing cell design, although particles in the range 0.6-0.83 mm transported readily within the cell. The gas-atomized coarse zinc powder (0.6-0.83 mm sieve) (Noranda) showed the most fluid properties, and fed continuously from hopper into cell at a rate proportional to discharge (measured in amp-hours). Thus all three techniques produce fuel consistent with the operation of the self-feeding cell, given appropriate size.

4. *Negligible Cell Shorting during Refueling.* The discharge of adjacent cells by shorting under oxygen-depleted conditions is severely impeded by cell polarization and inter-particle resistance of the bed. The contribution to energy loss is negligible: 0.02% of cell capacity is lost per recharge. The contributions to heat balance, hydrogen hazards, electrical safety, etc., are likewise found to be insignificant.

5. *Self discharge.* Self discharge of the zinc/air cell, resulting from the corrosion of zinc in contact with the metal anode current collector and basket, is insignificant. At ambient temperature, the corrosion current (9.4 mA per cell) amounts to 1.7 % of capacity per month. At elevated temperatures (57 °C) following shutdown of an active battery, the corrosion loss is 33 mA, or <0.08% of cell capacity if this temperature is maintained overnight (12 hours).

6. *Energy balance using hydrogen recovery.* The use of hydrogen gas as an reactant at a gas-diffusion anode in electrolytic recovery of zinc ($ZnO + H_2 = Zn + H_2O$) reduces the electrolysis voltage by about 1.5 V (compared with inert anodes evolving oxygen according to $ZnO = Zn + \frac{1}{2}O_2$). This indicates that the total energy conversion efficiency of a hypothetical transportation system using zinc as a vector for natural gas energy is about 34% (natural gas HHV to battery terminals) and thus comparable to hydrogen-consuming fuel cells.

7. *Cost of shot production.* The cost of shot production by water freezing of molten zinc is 1.5-3 ¢/lb (3.3-6.6 ¢/kWh) above the cost of super purity zinc, according to one producer. This cost sets a baseline cost for fuel production for this or other zinc-air systems.

8. *Dimensional control and Vibration Effects.* In stationary cells in the laboratory, the current self-feeding cells (3 mm gaps) do not appear to accept particles of 1 mm dimensions or above, and even 0.8 mm particles may show difficulty in feeding if the particles are of spherical or planar shapes of high friction coefficient. Particles in the range of 0.5-0.75 mm (e.g., cut

wire) and 0.6-0.83 mm (gas-atomized coarse powder) tended to feed continuously. Vibrations are important in any friction-controlled, gravity-fed flow. A means of quantifying such vibrations whether produced by roadway shocks, pump impellers, or some other mechanical means, should be developed and used in future tests of these cells, so that rigorous comparisons can be made.

9. *Industrial input into fabrication.* Both Noranda and Eagle-Picher appear to have technologies which are sufficiently close to what is needed for these cells to warrant further feasibility studies. The spouted bed product also appears to be directly usable, if the particles are reduced in size to about 0.75 mm, or if the channel connecting hopper to cell, and the cell entry gap, is increased from the current 2.5 mm to 3.5-4.5 mm. The costs of producing the seed particles needs to be assessed for this process. The process also requires a large captive inventory of immature particles required to sustain the fluidized bed. Since shot production appears to be very low cost, this approach should be studied for production of a particulate zinc fuel in the range of 0.5-2 mm in a possible centralized recovery scheme.

Both the spouted-bed and the Eagle-Picher processes might be configured for operation by a fleet, using user owned and operated equipment located a the fleet's home base. This would eliminate the need for green-field industrial plants and a fuels distribution system. We recommend scaleup of the spouted bed process and further detailed examination of the Eagle-Picher process for supporting the refuelable battery.

Acknowledgments

Work performed under the auspices of the U.S. Department of Energy by the Lawrence Livermore National Laboratory under Contract W-7405-Eng-48.

We gratefully acknowledge the support of this project by the International Lead Zinc Research Organization. We also express our gratitude to Centre de Technologie Noranda (Quebec) for samples of zinc shot. We acknowledge and thank Eagle-Picher, Inc. (Joplin MO) for supplying compressed zinc plates, and for the many helpful discussions and suggestions from Dr. Robert Parker. We gratefully acknowledge samples of battery separators from Pall/RAI, Inc. Finally, we thank The Energy Manufacturing and Transportation Technology Program (LLNL) and Laboratory Directed Research and Development Program, which furnished cell plates and frames used in these tests, as well as supporting laboratory equipment.

References

1. John F. Cooper, Dennis Fleming, Douglas Hargrove, Ronald Koopman, and Keith Peterman, "A refuelable zinc/air battery for fleet electric vehicle propulsion," SAE Technical Paper 951948, in *Electric and Hybrid Vehicles--Implementation of Technology,* (SP-1105), August 7-10 1995.
2. John F. Cooper, "Continuous-feed electrochemical cell with non-packing particulate electrode," US Patent No. 5,434,010 July 18, 1995.
3. John F. Cooper "Apparatus and method for the production of zinc fuel particles by a combined electrochemical and mechanical process," US Patent pending.
4 . Private communication, Dwane Coates, Eagle-Picher Inc., Joplin MO; to John F. Cooper, LLNL; August 1995.

5. Private communication, Robert Parker, Eagle-Picher Inc., Joplin MO; to John F. Cooper, LLNL; March 1996.
6. Private communication from Huron Valley Steel, Bob Forgues Tel. (352) 697-3400 to John F. Cooper, LLNL, March 29 1996.
7. Frank Tokarz, J. Ray Smith, John Cooper, Don Bender, and Salvador Aceves, "A concept electric vehicle using zinc air and flywheel batteries," (*Proc. Electric and Hybrid Vehicle Technology '95*; UK and International Press, Dorking, Surrey, UK Oct. 2 1995). LLNL Preprint UCRL-JC-121700; October 2, 1995.
8. Frank Tokarz, J. Ray Smith, John Cooper and Salvador Aceves, "A zinc-air battery and flywheel zero emission vehicle," (Proc. Sustainable Transportation '95; Northeast Sustainable Energy Association, Rhode Island and Connecticut, Nov. 13-15, 1995). LLNL Preprint UCRL-JC-121727; October 3 1995.
9. J. W. Evans, *Spouted bed electroregeneration of zinc and electrolyte for refueled zinc-air batteries* (Final Report: ZB-1 Zinc-Air Batteries, for International Lead Zinc Research Organization, P.O. Box 12036, Research Triangle Park, NC 22709-4647; March 1996).

Appendix: Microphotographs of Zinc Particles Tested in this work.

Figure A1. Tested products. (A) 0.75 mm cut wire (Platt, Inc.); (B) particles grown in a spouted bed (UCB); (C) gas-atomized coarse powder (Centre de Technologie Noranda); and (D) chopped plates of compacted zinc fines (Eagle-Picher, Inc.) Scale is 0.5 mm, smallest division. Source of microphotographs: LLNL.

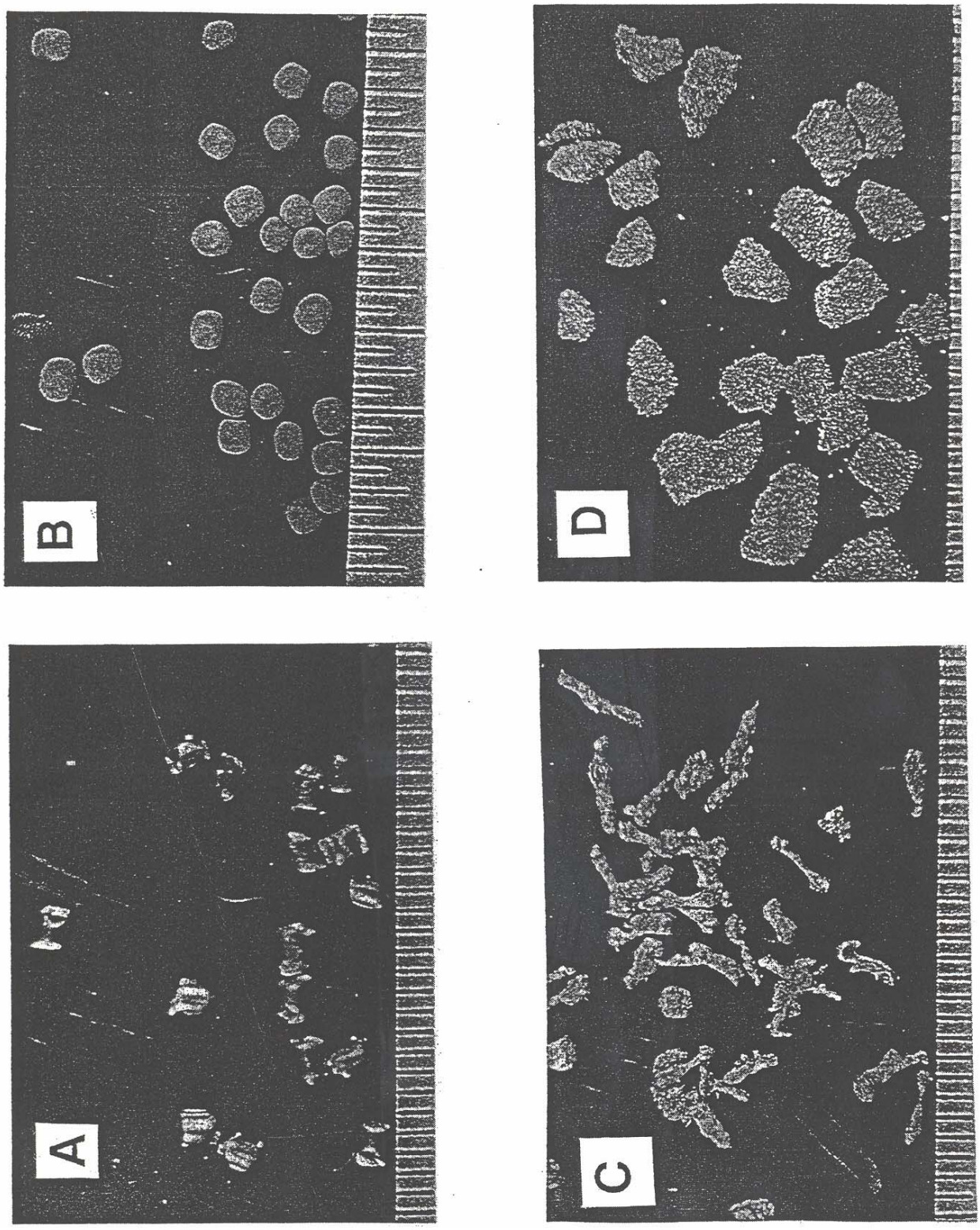
A
B
C
D